ACS Medicinal Chemistry Letters

pubs.acs.org/acsmedchemlett

Pharmacophore Refinement Guides the Design of Nanomolar-Range Botulinum Neurotoxin Serotype A Light Chain Inhibitors

Jonathan E. Nuss,[†,#] Yuxiang Dong,[‡,#] Laura M. Wanner,[†] Gordon Ruthel,[†] Peter Wipf,[§] Rick Gussio,[∥] Jonathan L. Vennerstrom,[‡] Sina Bavari,*[,†] and James C. Burnett*[,⊥]

[†]United States Army Medical Research Institute of Infectious Diseases, Frederick, Maryland 21702, [‡]Department of Pharmaceutical Sciences, College of Pharmacy, University of Nebraska Medical Center, Omaha, Nebraska 68198, [§]Department of Chemistry and Combinatorial Chemistry Center, University of Pittsburgh, Pittsburgh, Pennsylvania 15260, [∥]Developmental Therapeutics Program, National Cancer Institute at Frederick, Frederick, Maryland 21702, and [⊥]Target Structure-Based Drug Discovery Group, SAIC-Frederick, Inc., National Cancer Institute at Frederick, Frederick, Maryland 21702

ABSTRACT Botulinum neurotoxins (BoNTs) are the deadliest of microbial toxins. The enzymes' zinc(II) metalloprotease, referred to as the light chain (LC) component, inhibits acetylcholine release into neuromuscular junctions, resulting in the disease botulism. Currently, no therapies counter BoNT poisoning postneuronal intoxication; however, it is hypothesized that small molecules may be used to inhibit BoNT LC activity in the neuronal cytosol. Herein, we describe the pharmacophore-based design and chemical synthesis of potent [non-zinc(II) chelating] small molecule (nonpeptidic) inhibitors (SMNPIs) of the BoNT serotype A LC (the most toxic of the BoNT serotype LCs). Specifically, the three-dimensional superimpositions of 2-[4-(4-amidinephenoxy)-phenyl]indole-6-amidine-based SMNPI regioisomers [K_i = 0.600 μM (±0.100 μM)], with a novel lead bis-[3-amide-5-(imidazolino)phenyl]terephthalamide (BAIPT)-based SMNPI [K_i = 8.52 μM (±0.53 μM)], resulted in a refined four-zone pharmacophore. The refined model guided the design of BAIPT-based SMNPIs possessing K_i values = 0.572 (±0.041 μM) and 0.900 μM (±0.078 μM).

KEYWORDS Botulinum neurotoxin, small molecule inhibitor, gas-phase pharmacophore, rational design, biothreat agent

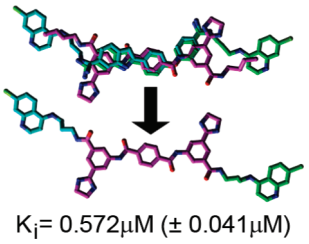

Botulinum neurotoxins (BoNTs) are the deadliest of known microbial toxins;[1] for example, it is estimated that a lethal BoNT dose (LD_{50}) for *Homo sapiens* is 1 ng kg^{-1} body mass.[1] As a result, these enzymes are classified as category A, highest priority biothreat agents by the Centers for Disease Control and Prevention.[2]

Secreted by strains of anaerobic bacillus *Clostridium botulinum*,[1] there are seven known BoNT serotypes (designated A–G). Serotypes A–C, E, and F cause human botulism.[3,4] The mechanism of BoNT neuronal intoxication can be summarized as follows:[1] (1) Postproteolytic activation, the enzyme consists of a disulfide-linked 100 kDa heavy chain (HC) and a 50 kDa light chain (LC); (2) the HC binds to neuronal cell surface receptors, triggering toxin internalization via an intracellular vesicle; (3) the HC mediates LC translocation out of the intracellular vesicle into the neuronal cytosol; and (4) the LC [a zinc (Zn)(II) metalloprotease] cleaves, depending on the serotype, one of three proteins (see below) composing the soluble *N*-ethylmaleimide-sensitive fusion protein attachment protein receptor (SNARE) complex. The SNARE complex negotiates the release of acetylcholine-containing synaptic vesicles into neuromuscular junctions. The toxin-induced inhibition of acetylcholine release, via the proteolysis of SNARE proteins, terminates neuron-to-muscle signaling, resulting in the life-threatening flaccid paralysis associated with botulism. The BoNT serotype A, E, and C LCs cleave synaptosomal-associated protein of 25 kDa (SNAP-25),[1] the BoNT serotype C LC also cleaves syntaxin,[1] and the BoNT serotype B, D, F, and G LCs cleave vesicle-associated membrane protein.[1]

Currently, there are no therapies available for the treatment of BoNT LC-mediated paralysis postneuronal intoxication. This is pivotal, as the current treatments for BoNT poisoning are limited to (1) the administration of antitoxin(s),[1,5] which is not effective postneuronal intoxication[6] and, therefore, would be of limited use following an act of bioterror (as it is likely that victims would seek medical attention only after enervation), and (2) mechanical ventilation, which is necessary once BoNT-induced paralysis compromises thoracic muscle contraction.[5] However, the latter form of treatment would also be impractical following even a limited act of bioterror employing a BoNT(s), as critical care resources would likely be overwhelmed.[7] Hence, there is considerable interest in discovering and developing small

Received Date: March 18, 2010
Accepted Date: June 21, 2010
Published on Web Date: June 24, 2010

DOI: 10.1021/ml100056v | *ACS Med. Chem. Lett.* **2010**, *1*, 301–305

molecules as therapeutics to inhibit BoNT LC proteolytic activity postneuronal intoxication.[1,8,9] Moreover, with respect to the development of small molecule therapeutics, the BoNT serotype A LC (BoNT/A LC) represents a top priority, as it, versus other BoNT LCs known to cause botulism in humans, possesses the longest duration of activity in the neuronal cytosol.[3,4] Thus, the hypothesis rationalizing a small molecule-based therapeutic approach for the treatment of BoNT/A LC intoxication is as follows: Small, druglike molecules can penetrate into the neuronal cytosol[10] and inhibit the toxin's LC proteolytic activity postneuronal intoxication. In turn, this mechanism would protect SNAP-25 and, hence, the function of the SNARE protein complex. Additionally, if stockpiled in dry, sunlight-free, temperature-controlled locations, chemically stable small molecules would remain viable for many years. In contrast, vaccines possess comparatively shorter shelf-lives.

Current X-ray structures of the BoNT/A LC fail to rationalize the structure−activity relationships (SAR) for our competitive, non-Zn(II) chelating, small molecule (nonpeptidic) inhibitors (SMNPIs) of the BoNT/A LC.[10−12] For this reason, we are successfully employing a gas-phase pharmacophore-based approach for SMNPI discovery and optimization.[11,12] This paradigm uses an efficient, iterative approach: SMNPIs are continually integrated into the pharmacophore to both develop three-dimensional (3D) search queries to discover novel SMNPI chemotypes (via the 3D database mining of small molecule libraries) and guide the rational design of more potent SMNPI derivatives. Following, structure−activity data from both database-mined and rationally designed SMNPIs are incorporated back into the model, resulting in further pharmacophore refinement.[10−13]

Employing this strategy, we recently reported a three-zone iteration of the pharmacophore for BoNT/A LC inhibition[11] that guided the design of 2-[4-(4-amidinephenoxy)phenyl]indole-6-amidine (2,4,4-APPIA)-based SMNPI regioisomers **1a** and **1b** (Table 1).[11] In vitro testing of **1a** and **1b** indicated that the regioisomers possess a K_i = 0.600 μM (±0.100 μM). However, it is important to note that the substituted bis-amidine moieties of **1a** and **1b** are not chemically stable during high-performance liquid chromatography (HPLC) separation, which prohibits regioisomer isolation. Additionally, the selective syntheses of individual regioisomers **1a** and **1b** are also prohibitive; therefore, we are currently exploring alternative cationic moieties to further advance the development and the optimization of this chemotype. Furthermore, we have reported how the three-zone pharmacophore was employed to generate a 3D search query that identified novel bis-[3-amide-5-(imidazolino)phenyl]terephthalamide (BAIPT)-based SMNPI **2** (Table 1),[12] a lead inhibitor possessing a K_i = 8.52 μM (±0.53 μM). The discovery of **2** was particularly compelling because one of its bis-butylamide substituents is located outside of the three-zone iteration of the pharmacophore,[12] implying the possibility of a fourth zone of SMNPI occupancy (Figure 1a). Importantly, a new pharmacophore zone 4 could potentially be exploited to discover new SMNPI chemotypes, as well as guide the synthetic optimization of our known SMNPIs.

To initially examine the possibility of a four-zone pharmacophore, sterically feasible intramolecular conformations of

Table 1. SMNPI Two-Dimensional Structures and Inhibition Constants

SMNPI	STRUCTURE & K_i Value
1a & **1b**	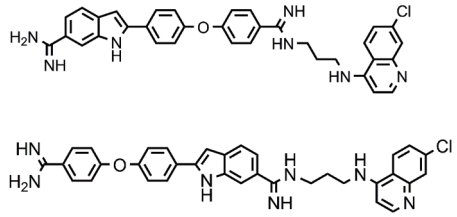 K_i = 0.600μM (+/- 0.100μM)[11 a]
2	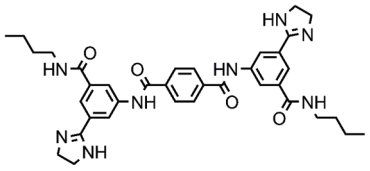 K_i = 8.52μM (+/- 0.53μM)
3	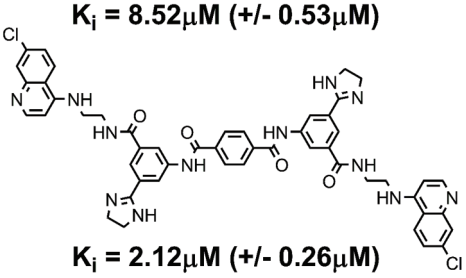 K_i = 2.12μM (+/- 0.26μM)
4	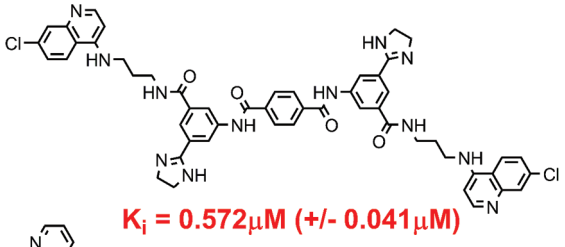 K_i = 0.572μM (+/- 0.041μM)
5	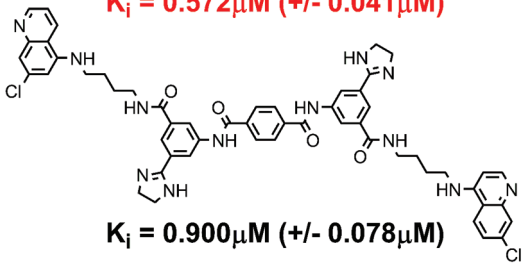 K_i = 0.900μM (+/- 0.078μM)

[a] Published K_i value (ref 11).

1a, **1b**, and **2** were superimposed in gas phase. As shown in Figure 2a, the SMNPIs overlaid with good chemical complementarity. Of particular significance to pharmacophore refinement, the 4-amino-7-chloroquinoline (4,7-ACQ) components of **1a** and **1b** and the terminal methylenes of the butylamide substituents of **2** can occupy proximal locations within empirically verified zone 3[11] and hypothesized pharmacophore zone 4, respectively (Figure 2a) (with the 4,7-ACQ components providing greater zonal occupancy).

DOI: 10.1021/ml100056v | ACS Med. Chem. Lett. 2010, 1, 301–305

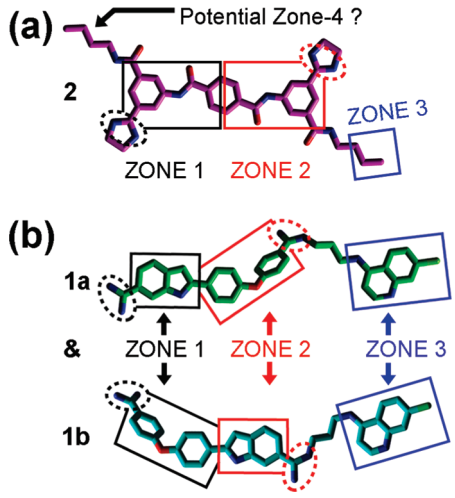

Figure 1. SMNPI alignments in a previously reported three-zone iteration of the pharmacophore for BoNT/A LC inhibition.[11,12] Chlorine atoms are light green, nitrogen atoms are blue, and oxygen atoms are red. Squares indicate planar pharmacophore components, and dashed spheres indicate cationic pharmacophore components. (a) SMNPI **2** (magenta carbons) as it was previously predicted to fit within the three-zone iteration of the pharmacophore.[12] (b) SMNPI regioisomers **1a** (green carbons) and **1b** (cyan carbons) were previously predicted to fit the three-zone pharmacophore such that their "core" 2,4,4-APPIA components oriented in opposite directions within zones 1 and 2, and as a result, their 4,7-ACQ substructures occupied only zone 3.[11]

Additionally, with respect to model refinement, the new SMNPI superimpositions are in contrast to our previously published three-zone pharmacophore,[11] which predicted that the 4,7-ACQ components of **1a** and **1b** occupy only zone 3 of this model (Figure 1b).

Further supporting a four-zone pharmacophore model are the superimpositions of the SMNPIs within the requirements of reported zones 1 and 2 (Figure 2a).[11,12] Specially, in zone 1 (Figure 2a), (1) the cationic amidines of **1a** and **1b** and the cationic imidazoline of **2** are located in close proximity and possess comparable directional orientations, (2) the hydrogen bond-donating indole nitrogens of **1a** and **1b** superimpose with a hydrogen bond-donating amide nitrogen of the "core" terephthalamide of **2**, (3) the phenyl components of the indoles of **1a** and **1b** align closely with the zone 1-occupying phenyl of **2**, and (4) the central phenyls of **1a** and **1b** superimpose with the terephthalamide phenyl of **2**. It is notable that in the refined four-zone pharmacophore (Figure 2a) versus the three-zone iteration of the model (Figure 1), the central phenyl rings of **1a**, **1b**, and **2** form the key basis for SMNPI alignment and, therefore, are now included within the zone 1 planar component (reference Figure 1 vs Figure 2a). In zone 2 (Figure 2a), (1) the ether oxygens of **1a** and **1b** superimpose with, and are oriented in the same direction as, a terephthalamide carbonyl oxygen of **2**, (2) the terminal phenyls of **1a** and **1b** are located proximal to, and partially overlay with, the zone 2-occupying phenyl of **2**, and (3) the cationic amidines of **1a** and **1b** and the cationic imidazole of **2** align in good order and with equivalent directional orientations.

The 3D chemical complementarity observed for **1a**, **1b**, and **2**, when aligned in the four-zone pharmacophore

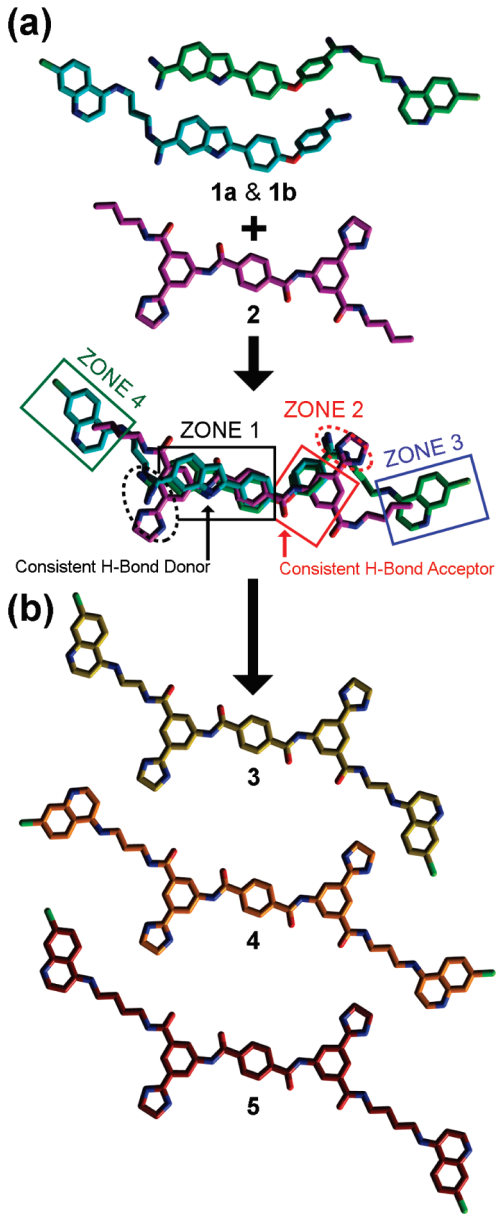

Figure 2. Three-dimensional alignments of SMNPIs **1a**, **1b**, and **2** in the context of the refined four-zone pharmacophore for BoNT/A LC inhibition, and rational designs based on the new model. (a) All colors and shape definitions are as indicated in Figure 1. (b) Carbon atoms are yellow, orange, and burgundy for designs **3**, **4**, and **5**, respectively; all other atom colors are as indicated in Figure 1.

(Figure 2a), formed the basis for the design of derivatives to improve the inhibitory potency of the BAIPT-based SMNPI chemotype. Specifically, the four-zone pharmacophore indicated that tethering 4,7-ACQ substructures onto the terminal amide amines of the BAIPT chemotype "core" with alkyl linkers (see derivatives **3**–**5**, Figure 2b) would result in SMNPIs with improved inhibitory potencies. Additionally, as shown in Figure 2b, **3**–**5** were designed to provide SAR exploring the lengths of the alkyl chains [i.e., ethyls (**3**), propyls (**4**), and butyls (**5**)] tethering the 4,7-ACQ zones 3- and 4-occupying components

DOI: 10.1021/ml100056v | ACS Med. Chem. Lett. 2010, 1, 301–305

Scheme 1. Synthesis of BAIPT-Based SMNPIs **3**−**5**[a]

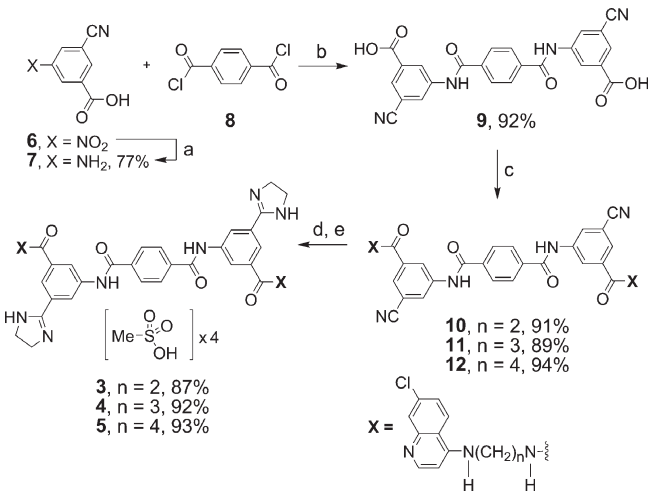

[a] Reagents and conditions: (a) Ammonium formate, 10% Pd−C, H_2O, 90 °C, 21 h, and then HCOOH. (b) DMAP, DMA, room temperature, 48 h. (c) N^1-(7-chloroquinolin-4-yl)-ethane-1,2-diamine (to provide **10**), N^1-(7-chloroquinolin-4-yl)-propane-1,3-diamine (to provide **11**), N^1-(7-chloroquinolin-4-yl)-butane-1,4-diamine (to provide **12**), HOBt, EDCI, DMA, room temperature, 24 h. (d) Ethylene diamine, NaSH, DMA, 120 °C, 2 h. (e) Methanesulfonic acid, CH_3CN, 70 °C, 0.5 h.

to the terminal amide amines of the BAIPT chemotype "core".

Scheme 1 displays the general synthetic procedure used to prepare **3**−**5**. Generation of the target compounds began with repeated attempts to reduce 3-cyano-5-nitrobenzoic acid (**6**) to corresponding aniline **7** via catalytic hydrogenation; however, substantial quantities of incomplete reduction products were constantly observed. To circumvent this obstacle, hydrogen transfer, rather than catalytic hydrogenation, was used to successfully generate **7** in 77% yield after acidification with formic acid and crystallization from water. Following, **7** and **8** were coupled using a modified procedure reported by Sellarajah et al.[14] to afford key intermediate **9** in 92% yield after quenching with water and crystallization from acetonitrile. Next, amide bond formation between **9** and the corresponding aminoquinolines[15] was performed at room temperature using HOBt and EDCI in DMA solvent to provide dinitrile intermediates **10**−**12**, respectively. The transformation of **10**−**12** into corresponding imidazoline targets **3**−**5** was achieved via reaction with ethylenediamine and NaSH in DMA solvent at 120 °C, employing a modified procedure of Sun et al.[16] Finally, the salts of **3**−**5** were obtained by stirring with methanesulfonic acid in acetonitrile at 70 °C. Detailed synthetic procedures and compound characterizations are provided as Supporting Information.

The K_i values for **3**−**5** (Table 1) were determined using a well-documented HPLC-based assay.[17−22] The four-zone pharmacophore-based designs were all more potent than **2** [K_i = 8.52 μM (±0.53 μM)]. Specifically, **3**−**5** possess K_i values of 2.12 (±0.26 μM), 0.572 (±0.041 μM), and 0.900 μM (±0.078 μM), respectively (Table 1). Furthermore, plots of the inhibition kinetics data for **3**−**5** indicate that all are competitive inhibitors (Supporting Information, Figures S1−S3), and additional in vitro analyses of the SMNPIs in the presence of Zn(II) concentrations equaling 5, 10, 25, and 50 μM did not effect inhibitory efficacies (Supporting Information, Table S1), thereby indicating that the SMNPIs do not chelate the Zn(II) of the enzyme's catalytic engine. The in vitro results obtained for **3**−**5** (Table 1) confirm the presence of pharmacophore zone 4. Moreover, the increased inhibitory potencies of **3**−**5**, versus **2**, demonstrate that, with each refinement of the gas-phase pharmacophore, the model's predictive resolution is improved and that it can be used to design more potent SMNPIs.

On the basis of the SAR provided by **3**−**5**, the inhibitory potency of **4** implies that the optimal length of the alkyl tether connecting SMNPI components is a propyl chain. By contrast, the inhibitory potency of **3** indicates that shorter ethyl tethers do not allow the SMNPI's 4,7-ACQ moieties to achieve optimal zones 3 and 4 occupancy, while the inhibitory potency of **5** indicates that longer butyl tethers overextend optimal 4,7-ACQ binding in zones 3 and 4. To provide SAR that will further guide SMNPI optimization (in vitro), future BAIPT-based designs will not only explore the effects of modified tethers (e.g., linkers with increased rigidity and the inclusion of heteroatoms) on BoNT/A LC inhibition, but will also incorporate a diversity of zone 3- and zone 4-occupying components (e.g., indoles, phenyls, pyridines, etc.). Furthermore, future studies will also be conducted to examine BAIPT-based SMNPI SNAP-25 protection and toxicity in neurons.

In summary, our gas-phase pharmacophore for BoNT/A LC inhibition is constantly enabling the rational design of more potent SMNPIs. In the current study, a refined four-zone iteration of the model was generated via the 3D superimposition of two different SMNPI chemotypes. To empirically validate the refined model, three target compounds based on the BAIPT chemotype "core" were synthesized and examined in vitro. Of the three designs, all are more potent than parent compound **2**, while **4** is the most potent non-Zn(II)-chelating, nonhydroxamic acid-containing, SMNPI of the BoNT/A LC reported to date. Moreover, comparison of the inhibitory potencies of **1a**, **1b**, and **4** indicates that a propyl tether may be optimal for accessing pharmacophore zones 3 and 4 with an aromatic moiety. In general, the refined pharmacophore model forms the basis for increasing the activities of our non-Zn(II)-chelating SMNPI chemotypes. Future four-zone pharmacophore-based designs will focus on developing SAR to provide strategies for optimizing the chemical and steric compositions of SMNPI components populating zones 3 and 4 (e.g., the 4,7-ACQ components of **1a**, **1b**, and **3**−**5**), as well as the flexibility/rigidity and composition of the tethers linking zones 1 and 4 and zones 2 and 3 (e.g., the propyl linkers of **4**).

SUPPORTING INFORMATION AVAILABLE

Descriptions of molecular modeling techniques employed for pharmacophore refinement, general chemistry methods, experimental details for the syntheses and characterization of **3**−**5**, **7**, and **9**−**12**, and inhibition assay conditions and K_i value determination. This material is available free of charge via the Internet at http://pubs.acs.org.

AUTHOR INFORMATION

Corresponding Author: *To whom correspondemce should be addressed. (S.B.) Tel: 301-619-4246. Fax: 301-619-2348.

DOI: 10.1021/ml100056v | *ACS Med. Chem. Lett.* **2010**, *1*, 301–305

E-mail: sina.bavari@us.army.mil. (J.C.B.) Tel: 804-225-0527. Fax: 804-828-8556. E-mail: burnettjames@mail.nih.gov.

Author Contributions: # The authors contributed equally to this work.

Funding Sources: The presented research was supported by Defense Threat Reduction Agency project 3.10084_09_RD_B and also Agreement Y3CM 100505 (MRMC and NCI, National Institutes of Health) for J.C.B. Furthermore, for J.C.B., in accordance with SAIC-Frederick, Inc., contractual requirements, this project has been funded in whole or in part with federal funds from the National Cancer Institute, National Institutes of Health, under Contract HHSN261200800001E.

Notes: The authors report no conflicts of interest in this work. The content of this publication does not necessarily reflect the views or policies of the Department of Health and Human Services, nor does mention of trade names, commercial products, or organizations imply endorsement by the U.S. Government or the U.S. Army.

ABBREVIATIONS 4,7-ACQ, 4-amino-7-chloroquinoline; 2,4,4-APPIA, 2-[4-(4-amidinephenoxy)phenyl]indole-6-amidine; BAIPT, bis-[3-amide-5-(imidazolino)phenyl]terephthalamide; BoNT/A LC, botulinum neurotoxin serotype A light chain; SMNPI, small molecule (nonpeptidic) inhibitor.

REFERENCES

(1) Willis, B.; Eubanks, L. M.; Dickerson, T. J.; Janda, K. D. The Strange Case of the Botulinum Neurotoxin: Using Chemistry and Biology to Modulate the Most Deadly Poison. *Angew. Chem., Int. Ed. Engl.* **2008,** *47*, 8360–8379.

(2) http://emergency.cdc.gov/agent/agentlist-category.asp.

(3) Foran, P. G.; Davletov, B.; Meunier, F. A. Getting Muscles Moving Again After Botulinum Toxin: Novel Therapeutic Challenges. *Trends Mol. Med.* **2003,** *9*, 291–299.

(4) Foran, P. G.; Mohammed, N.; Lisk, G. O.; Nagwaney, S.; Lawrence, G. W.; Johnson, E.; Smith, L.; Aoki, K. R.; Dolly, J. O. Evaluation of the Therapeutic Usefulness of Botulinum Neurotoxin B, C1, E, and F Compared with the Long Lasting Type A. Basis for Distinct Durations of Inhibition of Exocytosis in Central Neurons. *J. Biol. Chem.* **2003,** *278*, 1363–1371.

(5) Arnon, S. S.; Schechter, R.; Inglesby, T. V.; Henderson, D. A.; Bartlett, J. G.; Ascher, M. S.; Eitzen, E.; Fine, A. D.; Hauer, J.; Layton, M.; Lillibridge, S.; Osterholm, M. T.; O'Toole, T.; Parker, G.; Perl, T. M.; Russell, P. K.; Swerdlow, D. L.; Tonat, K. Botulinum Toxin as a Biological Weapon: Medical and Public Health Management. *J. Am. Med. Assoc.* **2001,** *285*, 1059–1070.

(6) Smith, T. J.; Lou, J.; Geren, I. N.; Forsyth, C. M.; Tsai, R.; Laporte, S. L.; Tepp, W. H.; Bradshaw, M.; Johnson, E. A.; Smith, L. A.; Marks, J. D. Sequence Variation within Botulinum Neurotoxin Serotypes Impacts Antibody Binding and Neutralization. *Infect. Immun.* **2005,** *73*, 5450–5457.

(7) Wein, L. M.; Liu, Y. Analyzing a Bioterror Attack on the Food Supply: The Case of Botulinum Toxin in Milk. *Proc. Natl. Acad. Sci. U.S.A.* **2005,** *102*, 9984–9989.

(8) Cai, S.; Singh, B. R. Strategies to Design Inhibitors of Clostridium Botulinum Neurotoxins. *Infect. Disord.: Drug Targets* **2007,** *7*, 47–57.

(9) Capkova, K.; Salzameda, N. T.; Janda, K. D. Investigations into Small Molecule Non-Peptidic Inhibitors of the Botulinum Neurotoxins. *Toxicon* **2009,** *54*, 575–582.

(10) Burnett, J. C.; Ruthel, G.; Stegmann, C. M.; Panchal, R. G.; Nguyen, T. L.; Hermone, A. R.; Stafford, R. G.; Lane, D. J.; Kenny, T. A.; McGrath, C. F.; Wipf, P.; Stahl, A. M.; Schmidt, J. J.; Gussio, R.; Brunger, A. T.; Bavari, S. Inhibition of Metalloprotease Botulinum Serotype A: From a Pseudo-Peptide Binding Mode to a Small Molecule that is Active in Primary Neurons. *J. Biol. Chem.* **2007,** *282*, 5004–5014.

(11) Burnett, J. C.; Wang, C.; Nuss, J. E.; Nguyen, T. L.; Hermone, A. R.; Schmidt, J. J.; Gussio, R.; Wipf, P.; Bavari, S. Pharmacophore-Guided Lead Optimization: the Rational Design of a Non-Zinc Coordinating, Sub-Micromolar Inhibitor of the Botulinum Neurotoxin Serotype a Metalloprotease. *Bioorg. Med. Chem. Lett.* **2009,** *19*, 5811–5813.

(12) Hermone, A. R.; Burnett, J. C.; Nuss, J. E.; Tressler, L. E.; Nguyen, T. L.; Solaja, B. A.; Vennerstrom, J. L.; Schmidt, J. J.; Wipf, P.; Bavari, S.; Gussio, R. Three-Dimensional Database Mining Identifies a Unique Chemotype that Unites Structurally Diverse Botulinum Neurotoxin Serotype A Inhibitors in a Three-Zone Pharmacophore. *ChemMedChem* **2008,** *3*, 1905–1912.

(13) Burnett, J. C.; Opsenica, D.; Sriraghavan, K.; Panchal, R. G.; Ruthel, G.; Hermone, A. R.; Nguyen, T. L.; Kenny, T. A.; Lane, D. J.; McGrath, C. F.; Schmidt, J. J.; Vennerstrom, J. L.; Gussio, R.; Solaja, B. A.; Bavari, S. A Refined Pharmacophore Identifies Potent 4-Amino-7-Chloroquinoline-Based Inhibitors of the Botulinum Neurotoxin Serotype A Metalloprotease. *J. Med. Chem.* **2007,** *50*, 2127–2136.

(14) Sellarajah, S.; Lekishvili, T.; Bowring, C.; Thompsett, A. R.; Rudyk, H.; Birkett, C. R.; Brown, D. R.; Gilbert, I. H. Synthesis of Analogues of Congo Red and Evaluation of Their Anti-Prion Activity. *J. Med. Chem.* **2004,** *47*, 5515–5534.

(15) Natarajan, J. K.; Alumasa, J. N.; Yearick, K.; Ekoue-Kovi, K. A.; Casabianca, L. B.; de Dios, A. C.; Wolf, C.; Roepe, P. D. 4-N-, 4-S-, and 4-O-Chloroquine Analogues: Influence of Side Chain Length and Quinolyl Nitrogen pKa on Activity Versus Chloroquine Resistant Malaria. *J. Med. Chem.* **2008,** *51*, 3466–3479.

(16) Sun, M.; Wei, H.-T.; Li, D.; Zheng, Y.-G.; Cai, J.; Ji, M. Mild and Efficient One-Pot Synthesis of 2-Imidazolines from Nitriles Using Sodium Hydrosulfide as Catalyst. *Synth. Commun.* **2008,** *38*, 3151–3158.

(17) Schmidt, J. J.; Bostian, K. A. Endoproteinase Activity of Type A Botulinum Neurotoxin: Substrate Requirements and Activation by Serum Albumin. *J. Protein Chem.* **1997,** *16*, 19–26.

(18) Schmidt, J. J.; Bostian, K. A. Proteolysis of Synthetic Peptides by Type A Botulinum Neurotoxin. *J. Protein Chem.* **1995,** *14*, 703–708.

(19) Schmidt, J. J.; Stafford, R. G. Fluorigenic Substrates for the Protease Activities of Botulinum Neurotoxins, Serotypes A, B, and F. *Appl. Environ. Microbiol.* **2003,** *69*, 297–303.

(20) Schmidt, J. J.; Stafford, R. G. A High-Affinity Competitive Inhibitor of Type A Botulinum Neurotoxin Protease Activity. *FEBS Lett.* **2002,** *532*, 423–426.

(21) Schmidt, J. J.; Stafford, R. G.; Bostian, K. A. Type A Botulinum Neurotoxin Proteolytic Activity: Development of Competitive Inhibitors and Implications for Substrate Specificity at the S1' Binding Subsite. *FEBS Lett.* **1998,** *435*, 61–64.

(22) Schmidt, J. J.; Stafford, R. G.; Millard, C. B. High-Throughput Assays for Botulinum Neurotoxin Proteolytic Activity: Serotypes A, B, D, and F. *Anal. Biochem.* **2001,** *296*, 130–137.

DOI: 10.1021/ml100056v | *ACS Med. Chem. Lett.* **2010,** *1*, 301–305